Inorg. Chem. **2004**, *43*, 2745–2753

Are Gas-Phase Reactions of Five-Coordinate Divalent Metal Ion Complexes Affected by Coordination Geometry?

Marianny Y. Combariza, Justin T. Fermann, and Richard W. Vachet*

Department of Chemistry, University of Massachusetts, Amherst, Massachusetts 01003

Received December 19, 2003

Five-coordinate metal complex ions of the type $[ML]^{2+}$ [where M = Mn(II), Fe(II), Co(II), Ni(II), Cu(II), Zn(II) and L= 1,9-bis(2-pyridyl)-2,5,8-triazanonane (DIEN-$(pyr)_2$) and 1,9-bis(2-imidazolyl)-2,5,8-triazanonane (DIEN-$(imi)_2$] have been reacted with acetonitrile in the gas phase using a modified quadrupole ion trap mass spectrometer. The kinetics and thermodynamics of these reactions show that the reactivity of these complexes is affected by metal electronic structure and falls into three groups: Mn(II) and Ni(II) complexes are the most reactive, Fe(II) and Co(II) complexes exhibit intermediate reactivity, and Cu(II) and Zn(II) complexes are the least reactive. To help explain the experimental trends in reactivity, theoretical calculations have been used. Due to the relatively large size of the metal complexes involved, we have utilized a two-layered ONIOM method to perform geometry optimizations and single point energy calculations for the $[ML]^{2+}$ and $[ML + CH_3CN]^{2+}$ systems. The calculations show that the reactant five-coordinate complexes ($[ML]^{2+}$) exhibit structures that are slightly distorted trigonal bipyramidal geometries, while the six-coordinate complexes ($[ML + CH_3CN]^{2+}$) have geometries that are close to octahedral. The ΔG values obtained from the ONIOM calculations roughly agree with the experimental data, but the calculations fail to completely explain the trends for the different metal complexes. The failure to consider all possible isomers as well as adequately represent π–d interactions for the metal complexes is the likely cause of this discrepancy. Using the angular overlap model (AOM) to obtain molecular orbital stabilization energies (MOSE) also fails to reproduce the experimental trends when only σ interactions are considered but succeeds in explaining the trends when π interactions are taken into account. These results indicate that the π-donor character of the CH_3CN plays a subtle, yet important, role in controlling the reactivity of these five-coordinate complexes. Also, the AOM calculations are consistent with the experimental data when the $[ML]^{2+}$ complexes have high-spin trigonal bipyramidal configurations. Generally, these results suggest that ion–molecule reactions can be very sensitive to metal complex coordination geometry and thus may have some promise for providing gas-phase coordination structure.

Introduction

The gas phase represents a unique environment in which the intrinsic interactions between metal ions and ligands can be studied undisturbed by the presence of solvent or counterions. The gas-phase coordination chemistry of transition metal ions and their complexes has been extensively studied, and comprehensive reviews are available.[1−3] One common means of gathering information about the gas-phase chemistry of metal ions and their complexes is to observe the chemistry as a function of the metal center. Periodic trends in reactivity,[4−9] bond dissociation energies,[10−12] and gas-phase structure[13,14] have provided tremendous insight into

* To whom correspondence should be addressed. E-mail: rwvachet@chem.umass.edu. Phone: (413) 545-2733. Fax: (413) 545-4490.

(1) *Organometallic Ion Chemistry*; Freiser, B. S., Ed.; Kluwer: Dordrecht, 1996.
(2) Eller, K.; Schwarz, H. *Chem. Rev.* **1991**, *91*, 1121−1177.
(3) Fisher K. J. *Prog. Inorg. Chem.* **2001**, *50*, 343−432.
(4) Freiser, B. S. *J. Mass Spectrom.* **1996**, *31*, 703−715.
(5) Allison, J. *Prog. Inorg. Chem.* **1986**, *34*, 627−676.
(6) Weis, P.; Kemper, P. R.; Bowers, M. T. *J. Phys. Chem. A* **1997**, *101*, 2809−2816.
(7) Kemper, P. R.; Weis, P.; Bowers, M. T. *Chem. Phys. Lett.* **1998**, *293*, 503−510.
(8) Kemper, P. R.; Weis, P.; Bowers, M. T.; Maitre, P. *J. Am. Chem. Soc.* **1998**, *120*, 13494−13502.
(9) Armentrout, P. B.; Georgiadis, R. *Polyhedron* **1988**, *7*, 1573−1581.
(10) Armentrout, P. B.; Halle, L. F.; Beauchamp, J. L. *J. Am. Chem. Soc.* **1981**, *103*, 6501−6502.
(11) Clemmer, D. E.; Armentrout, P. B. *J. Phys. Chem* **1991**, *95*, 3084−3090.
(12) Nanayakkara, V. K.; Freiser, B. S. *J Mass Spectrom.* **1997**, *32*, 475−482.
(13) Babinec, S. J.; Allison, J. *J. Am. Chem. Soc.* **1984**, *106*, 7718−7720.

10.1021/ic0354668 CCC: $27.50
Published on Web 03/24/2004

how metal electronic structure affects the inherent chemistry of metal complexes.

While this work has been immensely informative, most of the studies have been carried out with metals in the +1 oxidation state. This oxidation state makes drawing comparisons with solution chemistry difficult because in solution most transition metals are found in higher oxidation states. Higher oxidation states are common for late first row transition metals, Mn to Cu, which exhibit stable +2 states in the condensed phase. The recent development and application of several ionization techniques now allow the chemistry of metals in higher oxidation states and their complexes to be studied in the gas phase. The most widely used of these techniques is electrospray ionization, but other techniques, including the "pick-up" technique[15−17] and charge-stripping techniques,[18] have allowed the complexes of divalent metals to be studied in the gas phase, too. The ability to generate metal complexes in higher oxidation states has instigated numerous studies into the microsolvation of metal ions with both protic[19−22] and aprotic[20,23,24] solvents. Also, generating metals in higher oxidation states has been of analytical utility as metal complexes of organic molecules,[25] monosaccharides,[26−28] and peptides[29−31] have been shown to provide different, and sometimes more structurally useful, dissociation patterns.

Ion−molecule reactions of complexes having metals in higher oxidation states have also been studied because of their analytical and fundamental utility. Our group has begun to investigate the potential of using ion−molecule reactions to gather information such as coordination number and coordination structure from metal complexes.[32−35] Initial studies show that coordinatively unsaturated metal complexes readily react to add reagent gases such as water, ammonia, acetonitrile, and pyridine. The total number of reagent gas molecules added can then be related to the coordination number of the initial complex.[32] In addition, the kinetics and thermodynamics of these reactions can be telling about the functional groups bound to the metal.[35]

In more fundamental studies, gas-phase reactions of divalent metal complexes have provided some insight into the intrinsic (i.e., solvent-free) chemistry of complexes. For example, coordinatively unsaturated $[M(bpy)_2]^{2+}$ complexes, where M = Cr, Ru, Os and bpy is 2,2′-bipyridine, were reacted with O_2 to help understand the activation of molecular oxygen. These studies indicate that upon addition of O_2 to each of these complexes only Os(II) undergoes a formal oxidation to Os(VI) with a concomitant four-electron reduction of O_2, while the oxidation states of Cr and Ru are unaffected.[36] Other studies by the same group have investigated the competition between proton transfer and ligand exchange in the reactions of $M(CH_3OH)_n^{2+}$ (M = Fe, Mn) and $M(H_2O)_n^{2+}$ (M = Mn, Cu) with NH_3 and D_2O, and parallels to solution chemistry were observed.[37,38] Chen and co-workers have used electrospray to generate organometallic complexes of Ir[39,40] and Ru,[41] and reactions of these complexes with neutrals have provided insight into the mechanisms of C−H bond activation and olefin metathesis, respectively. The effects of axial ligation on the reactivity of Mn−salen complexes, particularly metal−oxo species, have also been studied in order to better understand the involvement of these species in epoxidation reactions.[42,43] The latter studies demonstrate the utility of gas-phase reactions for studying species that are too short-lived in solution or for studying reactions without the sometimes confounding effects of solvent.

We are interested in studying the gas-phase ligation reactions that divalent metal complexes with multidentate ligands undergo because of the intrinsic information that these reactions might provide. For example, these reactions might provide structural and thermodynamic information that when compared to solution or solid-state complexes might highlight the effects of solvent and crystal packing forces on metal complex structure. In this study, we investigate the impact of electronic structure on the reactions of five-coordinate complexes. We are specifically interested in determining how sensitive ion−molecule reactions are to

(14) Gapeev, A.; Yang, C. N.; Klippenstein, J.; Dunbar, R. C. *J. Phys. Chem. A* **2000**, *104*, 3246−3256.
(15) Woodward, C. A.; Dobson, M. P.; Stace, A. J. *J. Phys. Chem. A* **1996**, *100*, 5605−5607.
(16) Woodward, C. A.; Dobson, M. P.; Stace, A. J. *J. Phys. Chem. A* **1997**, *101*, 2279−2287.
(17) Stace, A. J. *J. Phys. Chem. A* **2002**, *106*, 7993−8005.
(18) Schroder, D.; Schwarz, H.; Wu, J.; Wesdemiotis, C. *Chem. Phys. Lett.* **2001**, *343*, 258−264.
(19) Blades, A. T.; Jayaweera, P.; Ikonomu, M. G.; Kebarle, P. *J. Chem. Phys.* **1990**, *92*, 5900−5906.
(20) Wright, R. R.; Walker, N. R.; Firth, S.; Stace, A. J. *J. Phys. Chem. A* **2001**, *105*, 54−64.
(21) Shvartsburg, A. A.; Siu, K. W. M. *J. Am. Chem. Soc.* **2001**, *123*, 10071−10075.
(22) Shvartsburg, A. A. *J. Am. Chem. Soc.* **2002**, *124*, 7910−7911.
(23) Kohler, M.; Leary, J. A. *Int. J. Mass Spectrom. Ion Processes* **1997**, *162*, 17−34.
(24) Seto, C.; Stone, J. A. *Int. J. Mass Spectrom. Ion Processes* **1998**, *175*, 263−276.
(25) Alvarez, E. J.; Vartanian, V. H.; Brodbelt, J. S. *Anal. Chem.* **1997**, *69*, 1147−1155.
(26) Smith, G.; Leary, J. A. *Int. J. Mass Spectrom.* **1999**, *193*, 153−160.
(27) Smith, G.; Kaffashan, A.; Leary, J. A. *Int. J. Mass Spectrom.* **1999**, *183*, 299−310.
(28) Desaire, H.; Leary, J. A. *Int. J. Mass Spectrom.* **2001**, *209*, 171−184.
(29) Hu, P.; Loo, J. A.; Smith, R. D. *J. Am. Soc. Mass Spectrom.* **1994**, *5*, 959−965.
(30) Hu, P.; Loo, J. A. *J. Am. Chem. Soc.* **1995**, *117*, 11314−11319.
(31) Lavanat, H.; Hecquet, E.; Hoppilliard, Y. *Int. J. Mass. Spectrom.* **1999**, *185*, 11−23.
(32) Vachet, R. W.; Hartman, J. R.; Callahan, J. H. *J. Mass Spectrom.* **1998**, *12*, 1209−1225.
(33) Vachet, R. W.; Callahan, J. H. *J. Mass Spectrom.* **2000**, *35*, 311−320.
(34) Vachet, R. W.; Hartman, J. R.; Gertner, J. W.; Callahan, J. H. *Int. J. Mass Spectrom.* **2001**, *204*, 102−112.
(35) Combariza, M. Y.; Vachet, R. W. *J. Am Soc. Mass Spectrom.* **2002**, *13*, 813−825.
(36) Molina-Svendsen, H.; Bojesen, G.; McKenzie, C. J. *Inorg. Chem.* **1998**, *37*, 1981−1983.
(37) Andersen, U. N.; Bojesen, G. *Int. J. Mass Spectrom. Ion Processes* **1996**, *153*, 1−7.
(38) Nielsen, S. B.; Bojesen, G. *Chem. Commun.* **1998**, *5*, 613−614.
(39) Hinderling, C.; Plattner, D. A.; Chen, P. *Angew. Chem., Int. Ed. Engl.* **1997**, *36*, 243−244.
(40) Hinderling, C.; Feichtinger, D.; Plattner, D. A.; Chen, P. *J. Am. Chem. Soc.* **1997**, *119*, 10793−10804.
(41) Hinderling, C.; Adlhart, P.; Chen, P. *Angew. Chem., Int. Ed.* **1998**, *37*, 2685−2689.
(42) Plattner, D. A.; Feichtinger, D.; El-Bahraoui, J.; Wiest, O. *Int. J. Mass Spectrom.* **2000**, *195*, 351−362.
(43) Feichtinger, D.; Plattner, D. A. *Angew. Chem. Int. Ed. Engl.* **1997**, *36*, 1718−1719.

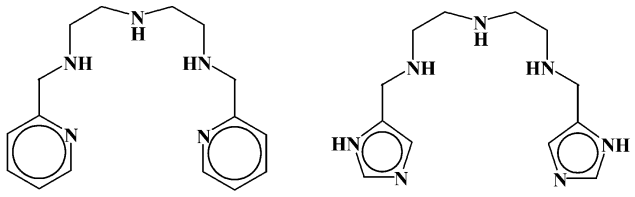

1,9-bis(2-pyridyl)-2,5,8-triazanonane
DIEN-(pyr)$_2$

1,9-bis(2-imidazolyl)-2,5,8-triazanonane
DIEN-(imi)$_2$

Figure 1. Ligand structures.

changes in the electronic structure of these complexes. Also of interest is whether ion−molecule reactions can provide any information about the coordination geometry of these complexes. Furthermore, because ligand substitution reactions of six-coordinate complexes in solution sometimes go through five-coordinate intermediates, a study of these intermediates without solvent might provide some interesting insight into these reactions. In particular, the potentially subtle effects of electronic differences might be clarified through the interpretation of our experimental data in light of *ab initio* and other electronic structure calculations.

Experimental Section

Instrumentation. A Bruker ESQUIRE-LC quadrupole ion trap mass spectrometer has been used in the current studies. The modifications made to the instrument in order to carry out the ion−molecule reaction studies have been reported previously,[35] but a brief overview of the experimental procedure is given here.

Acetonitrile and He are admitted into the vacuum system of the ESQUIRE-LC using two separate precision leak-valves that are connected to the vacuum manifold. The pressure inside the quadrupole ion trap is monitored using an ion gauge. The reading provided by the ion gauge is calibrated using the known deprotonation reaction rates of the 13^+, 12^+, and 11^+ charge states of ubiquitin with ammonia[44] (99.99%, Matheson Tri-gas, Parsippany, NJ). Correction factors from this calibration and the ion gauge sensitivity to CH_3CN[45] are then used to obtain the true gas pressure. The He buffer gas and CH_3CN pressures are monitored and kept at $1.0 \pm 0.3 \times 10^{-4}$ and $3.2 \pm 0.3 \times 10^{-7}$ Torr, respectively. The vacuum system temperature is monitored and maintained at 300 ± 2 K through all the experiments.

The metal complex ions of interest are selected and reacted with CH_3CN for different periods of time. The ion isolation process and the reaction time are controlled using the ESQUIRE-LC software. Kinetic data are obtained by monitoring the change in the intensity of the product and parent ions for up to 4000 ms. Equilibrium constants are calculated as a ratio of rate constants, which are determined by fitting the experimental data to a series of differential equations using the KinFit program.[46]

Ligand Synthesis. A description of the synthesis of the ligands in Figure 1 was described previously.[32,47] In short, either 2-pyridinecarboxaldehyde or 4(5)-imidazolecarboxaldehyde (Sigma-Aldrich, St. Louis, MO) is mixed with diethylenetriamine (DIEN) at a 2:1 (aldehyde/DIEN) ratio in anhydrous methanol. The mixture is then reacted for 24 h in a Parr shaking hydrogenator under a 60 psi atmosphere of H_2 (99.99%, Merriam-Graves, Springfield, MA) over Pd (10% Pd on carbon). The mixture is then filtered, and the final product is recovered as a yellow oil after allowing the solvent to evaporate.

Metal complexes are prepared by mixing equimolar amounts of $MnCl_2$, $FeCl_2$, $CoCl_2$, $NiCl_2$, $CuCl_2$, or $Zn(CH_3COO)_2$ solutions and the ligand of interest in methanol or water/methanol (1:1) to a final concentration of 50 μM. Complex ions are transferred to the gas-phase by ESI using a needle voltage of about 4 kV and a flow rate of 1.0−2.0 μL/min. Typically, a capillary temperature of 150 °C and a capillary exit offset voltage of 20−30 V are used.

Electronic Structure Calculations. Geometry optimizations followed by energy and vibrational frequency analyses were performed on the various metal−ligand complexes using the Gaussian suite of computational chemistry programs.[48] The electronic energies and vibrational frequencies were used to compute reaction free energies for the reaction adding a single CH_3CN ligand. It was impractical to use a fully quantum mechanical (QM) technique to describe the systems because of the large number of atoms in each complex and the usually open shell ground-state electronic configurations. We chose to use an embedding method,[49] implemented as the ONIOM[50] protocol in Gaussian, to take advantage of the natural separation between the electronically complex metal−ligand bonding, included in the "inner layer," and the relatively simple covalent bonding within the DIEN-based ligand, accounted in the "outer layer." The actual implementation of the ONIOM scheme involves not one but three calculations for each property, P; a high level calculation on the inner (I) layer, and low level calculations on the inner (I) layer and on the entire system (S). The results of these calculations are combined algebraically: $P(\text{ONIOM}) = P(\text{high}(I)) + [P(\text{low}(S)) - P(\text{low}(I))]$.[50,51] The implication of grouping the low level calculations is to suggest that we are correcting a high level calculation with the properties of the outer atoms computed at the low level of theory. The subtleties of terminating the inner layer with link atoms to avoid dangling bonds in QM electronic structure calculations are detailed elsewhere.[50]

In our work, we have found that the M(DIEN-(pyr)$_2$)$^{2+}$ complex is naturally partitioned by including the metal ion and all directly bonded nitrogen atoms in the inner layer and all other atoms in the outer layer with the exception of one carbon atom of each pyridine, which is needed to enforce sp^2 hybridization on the pyridyl nitrogen. When the additional ligand was introduced, the entire CH_3CN

(44) Zhang, X.; Cassady, C. *J. Am. Soc. Mass Spectrom.* **1996**, *7*, 1211−1218.
(45) Bartmess, J. E.; Georgiadis, R. M. *Vacuum* **1983**, *33*, 149−153.
(46) Shen, N. Z.; Pope, R. M.; Dearden, D. V. *Int. J. Mass Spectrom.* **2000**, *196*, 639−652.
(47) Harris, W. R.; Murase, I.; Timmons, J. H.; Martell, A. E. *Inorg. Chem.* **1978**, *17*, 889−894.
(48) Frisch, M. J.; Trucks G. W.; Schlegel, H. B.; Scuseria, G. E.; Robb, M. A.; Cheeseman, J. R.; Zakrzewski, V. G.; Montgomery Jr., J. A.; Vreven, T.; Kudin, K. N.; Burant, J. C.; Millam, J. M.; Iyengar, S. S.; Tomasi, J.; Barone, V.; Mennucci, B.; Cossi, M.; Scalmani, G.; Rega, N.; Petersson, G. A.; Nakatsuji, H.; Hada, M.; Ehara, M.; Toyota, K.; Fukuda, R.; Hasegawa, J.; Ishida, M.; Nakajima, T.; Honda, Y.; Kitao, O.; Nakai, H.; Klene, M.; Li, X.; Knox, J. E.; Hratchian, H. P.; Cross, J. B.; Adamo, C.; Jaramillo, J.; Gomperts, R.; Stratmann, R. E.; Yazyev, O.; Austin, A. J.; Cammi, R.; Pomelli, C.; Ochterski, J. W.; Ayala, P. Y.; Morokuma, K.; Voth, G. A.; Salvador, P.; Dannenberg, J. J.; Zakrzewski, V. G.; Dapprich, S., Daniels, A. D.; Strain, M. C.; Farkas, O.; Malick, D. K.; Rabuck, A. D.; Raghavachari, K.; Foresman, J. B.; Ortiz, J. V.; Cui, Q.; Baboul, A. G.; Clifford, S.; Cioslowski, J.; Stefanov, B. B.; Liu, G.; Liashenko, A.; Piskorz, P.; Komaromi, I.; Martin, R. L.; Fox, D. J.; Keith, T.; Al-Laham, M. A.; Peng, C. Y.; Nanayakkara, A.; Challacombe, M.; Gill, P. M. W.; Johnson, B.; Chen, W.; Wong, M. W.; Gonzalez, C.; Pople, J. A. *Gaussian03*, revision B.03; Gaussian, Inc.: Pittsburgh, PA, 2003.
(49) Gao, J. In *Reviews in Computational Chemistry*; Lipkowitz, K. B., Boyd, D. B., Eds.; VCH: New York, 1996; Vol. 7, p 119.
(50) Dapprich, S.; Komaromi, I.; Byun, K. S.; Morokuma, K.; Frisch, M. J. *THEOCHEM* **1999**, *461*, 1−21.
(51) Vreven, T.; Morokuma, K. *J. Comput. Chem.* **2000**, *21*, 1419−1432.

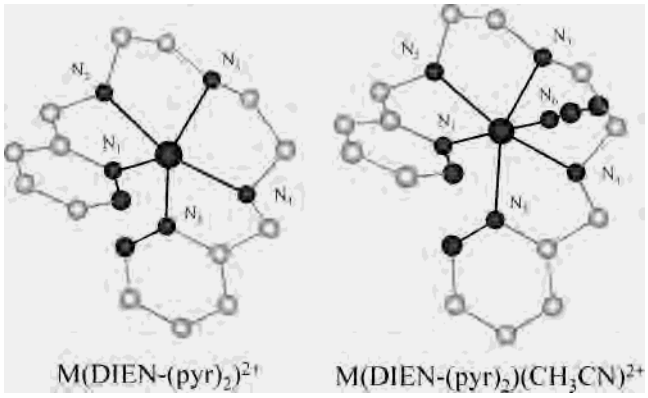

Figure 2. Partitioning scheme used in ONIOM calculations of M(DIEN-(pyr)$_2$)$^{2+}$ and M(DIEN-(pyr)$_2$)(CH$_3$CN)$^{2+}$. The atoms in black were treated using DFT, and the atoms in gray were treated using molecular mechanics. Refer to Figure 1 for atom connectivity in the ligands.

moiety was added to the inner layer. In this manner, reaction energies can be obtained from an ONIOM calculation on the reactant complex, the product complex, and a single analysis of the CH_3CN moiety performed at the high level of theory. For a pictorial representation of this partitioning scheme, see Figure 2. It is possible that this partitioning inadequately describes the π-character of the interactions between the metal ion and the pyridyl nitrogen, because the nitrogen so described is no longer part of a conjugated π-system in the high level calculations.[52] All outer layer atoms directly bonded to any atom in the inner layer were replaced with hydrogens as link atoms when performing calculations on the inner layer. We employed the Dreiding[53] molecular mechanics force field to model the interactions in the outer layer and a traditional basis set density functional method, specifically the B3LYP method[54−56] with the 6-311G(d,p) basis set,[57−59] to model the inner layer. The high level method is known to perform well for electronically complex metal ion containing molecules,[60−64] and the robustness of the ONIOM partitioning scheme was verified by comparison to fully QM calculations on the only closed shell example in our series, the Zn(DIEN-(pyr)$_2$)$^{2+}$ complex.

Results and Discussion

The ligands DIEN-(pyr)$_2$ and DIEN-(imi)$_2$ are pentadentate ligands, and consequently, we expected the formation of five-coordinate complexes with transition metal ions. On the basis of previous results,[32,35] five-coordinate complexes should add just a single CH_3CN molecule to fill the metal's coordination sphere, and indeed, this is the case for most complexes. For a few complexes, the addition of a second CH_3CN molecule is also observed to a small extent. This second CH_3CN either displaces one of the coordinating groups or adds as an outer-sphere ligand. At this point, our data do not allow us to distinguish between the two possibilities. Regardless of how the second CH_3CN is bound, its abundance is fairly insignificant and only exceeds 5% relative abundance for one complex (i.e., Ni(DIEN-(pyr)$_2$)$^{2+}$) even after a 4000 ms reaction time.

If the reactions of the various DIEN-(pyr)$_2$ and DIEN-(imi)$_2$ complexes are evaluated as a function of time, one notes that the reactions all achieve an equilibrium after about 2000 ms. Figure 3 displays typical kinetic plots for the reactions of Ni(DIEN-(imi)$_2$)$^{2+}$ and Cu(DIEN-(imi)$_2$)$^{2+}$ with CH_3CN. Clearly, there are significant differences between the two plots. The Cu(II) complex adds just one CH_3CN molecule, and the abundance ratio of the product ions to parent ions is less than 1. For the Ni(II) complex, the parent ion achieves a relative abundance of $<10\%$ after 2000 ms, and the product ion corresponding to the addition of one CH_3CN becomes the dominant ion. The kinetic data for these reactions can be fit by expression 1, and reaction rate constants can be determined.

$$ML^{2+} + CH_3CN \underset{k_2}{\overset{k_1}{\rightleftharpoons}} (ML + CH_3CN)^{2+} \qquad (1)$$

For each metal, the DIEN-(pyr)$_2$ complexes are more reactive with CH_3CN than the DIEN-(imi)$_2$ complexes. Table 1 shows the forward reaction rate (k_1) and equilibrium constants for the addition of one CH_3CN to each complex. Because the diethylenetriamine (DIEN) unit is the same in both ligands, differences in reactivity for a given metal are due to the differences in the coordinating ability of pyridine and imidazole. More efficient overlap of the donor atoms in imidazole, as compared to pyridine, likely causes the decreased reactivity seen in the complexes containing this functional group. In recent work, we showed that the types of functional groups in the ligand sphere can significantly impact the reactivity of metal complexes with CH_3CN. The reactivity of CH_3CN toward these complexes provides some insight into the electronic tuning of each metal by different coordination spheres.[35]

Of particular interest in this work is the reactivity trend that is observed upon changing the metal center that is coordinated to a given ligand. Table 1 clearly indicates that the reaction rate and equilibrium constants are markedly different for the complexes of each metal. The trend that is observed is Ni(II) > Mn(II) > Fe(II) > Co(II) > Cu(II) $\approx$ Zn(II). Also of note in Table 1 is that the equilibrium constants follow a very similar trend as the reaction rate constants. This is the case because the reactions of the complexes in Table 1 with CH_3CN are association reactions.

(52) Hall, R. J.; Hindle, S. A.; Burton, N. A.; Hillier, I. H. *J. Comput. Chem.* **2000**, *21*, 1433−1441.
(53) Mayo, S. L.; Olafson, B. D.; Goddard, W. A. *J. Phys. Chem.* **1990**, *94*, 8897−8909.
(54) Pople, J. A.; Head-Gordon, M.; Fox, D. J.; Raghavachari, K.; Curtiss, L. A. *J. Chem. Phys.* **1989**, *90*, 5622−5629.
(55) Curtiss, L. A.; Jones, C.; Trucks, G. W.; Raghavachari, K.; Pople, J. A. *J. Chem. Phys.* **1990**, *93*, 2537−2545.
(56) Becke, A. D. *J. Chem. Phys.* **1993**, *98*, 5648−5652.
(57) McLean, A. D.; Chandler, G. S. *J. Chem. Phys.* **1980**, *72*, 5639−5648.
(58) Krishnan, R.; Binkley, J. S.; Seeger, R.; Pople, J. A. *J. Chem. Phys.* **1980**, *72*, 650−654.
(59) Raghavachari, K.; Trucks, G. W. *J. Chem. Phys.* **1989**, *91*, 1062−1065.
(60) Tsipis, C. A. *Coord. Chem. Rev.* **1991**, *108*, 163−311.
(61) Wire, L. M.; Wheeler, S. D.; Wagenseller, E.; Marynick, D. S. *Inorg. Chem.* **1998**, *37*, 3099−3106 and references therein.
(62) Rulisek, L.; Havlas, Z. *J. Am. Chem. Soc.* **2000**, *122*, 10428−10439.
(63) Peschke, M.; Blades, A. T.; Kebarle, P. *J. Am. Chem. Soc.* **2000**, *122*, 10440−10449 and references therein.
(64) Marino, T.; Russo, N.; Sicilia, E.; Toscano, M.; Mineva, T. In *Advances in Quantum Chemistry*; Academic Press: New York, 2000; Vol. 36, pp 93−120 and references therein.

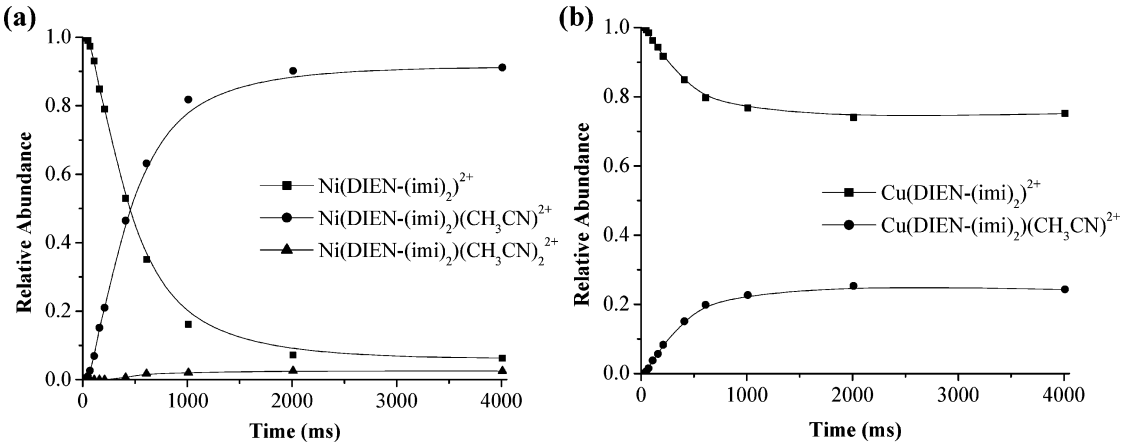

Figure 3. Typical kinetic plots obtained from the reactions of acetonitrile with (a) Ni(DIEN−(imi)$_2$)$^{2+}$ and (b) Cu(DIEN−(imi)$_2$)$^{2+}$.

Table 1. Rate (k_1) and Equilibrium Constants for the Addition of One Acetonitrile Molecule to the Metal Complexes of DIEN-(pyr)$_2$ and DIEN-(imi)$_2$

	rate constants ($\times 10^{-10}$ cm^3 molecule^{-1} s^{-1})[a]		equilibrium constants[b]	
metal	DIEN-(pyr)$_2$	DIEN-(imi)$_2$	DIEN-(pyr)$_2$	DIEN-(imi)$_2$
Mn	3.7 ± 0.5	2.0 ± 0.2	80 ± 30[c]	12 ± 4
Fe	3.1 ± 0.9	1.8 ± 0.4	20 ± 10	6 ± 2
Co	2.3 ± 0.4	1.0 ± 0.3	3.0 ± 1.5	1.4 ± 0.2
Ni	4.5 ± 1.0	2.5 ± 1.0	140 ± 60[c]	35 ± 15
Cu	0.9 ± 0.2	0.7 ± 0.3	0.9 ± 0.2	0.5 ± 0.1
Zn	0.8 ± 0.4	0.5 ± 0.2	0.6 ± 0.3	0.3 ± 0.1

[a] These values were obtained by fitting expression 1 to the experimental data. [b] Equilibrium constants were obtained from the equation $K = k_1/k_2$, where k_1 and k_2 are the values obtained by fitting expression 1 to the experimental data. [c] The fitting for these data failed to provide a value for k_2, so the equilibrium constant was estimated directly from mass spectra taken under equilibrium conditions.

Association reactions in the gas phase occur in two steps as shown in expressions 2 and 3.

$$ML^{n+} + CH_3CN \underset{k_b}{\overset{k_a}{\rightleftharpoons}} (ML + CH_3CN)^{n+}* \quad (2)$$

$$(ML + CH_3CN)^{n+}* + He \underset{k_{ac}}{\overset{k_s}{\rightleftharpoons}} (ML + CH_3CN)^{n+} + He \quad (3)$$

First, an excited intermediate is formed, and then, the intermediate can either dissociate back into reactants or form a detectable product after collisional stabilization by helium that is present in the vacuum system. The observed forward reaction rate constants will depend on the magnitude of k_a, k_b, k_s, and [He]. For the reactions of each metal complex, only k_b should vary significantly, and the magnitude of this value is related to the strength of the interaction between the metal complex and CH_3CN. Because the equilibrium constant is also related to the strength of this interaction, the reaction rate and equilibrium constants should follow a similar trend. The correlation between the rate and equilibrium constants is not expected to be perfect, though, because slight differences in the sizes of the various metal complex ions will cause k_a and k_s to be slightly different for each complex.

Presumably, the reactivity trend observed in Table 1 is a consequence of the differences in the electronic structure of each metal. A direct comparison to known solution chemistry, however, is problematic due to the ability of most solvents (e.g., water) to act as a ligand, which makes the chemistry of truly five-coordinate complexes in solution difficult to study. Five-coordinate complexes are expected to be intermediates in ligand substitution reactions of six-coordinate complexes that occur by purely dissociative mechanisms, but relatively few such intermediates have been studied. Thus, the current gas-phase studies might provide some insight into the effect of electronic structure on ligand substitution reactions.

An initial attempt to explain the trend shown in Table 1 involved consideration of the binding preferences of divalent metals for a given ligand. The so-called Irving−Williams series, which typically follows as Mn(II) < Fe(II) < Co(II) < Ni(II) < Cu(II) > Zn(II), is related to the decrease in ionic radii across the series. Decreased ionic radii usually lead to stronger metal−ligand bonds. Clearly, however, this series does not explain the trend observed in the current work. The low reactivity of Cu(II) can be explained by considering the Jahn−Teller distortion present in six-coordinate Cu(II) complexes. Similarly, the low reactivity of the Zn(II) complexes is likely a result of the metal−ligand repulsion caused by the closed-shell nature of Zn(II). The relatively high reactivity of the Mn(II) complexes, however, cannot be explained as easily. In order to determine if other geometric or electronic factors are responsible for the observed trends, electronic structure calculations were performed.

ONIOM Calculations. Numerous studies concerned with theoretical calculations of transition metal complexes have been carried out in recent years. It has been shown that DFT calculations can fairly efficiently provide accurate complex geometries and reaction energies for transition metal systems if the appropriate basis set is chosen.[60−64] In the current study, however, the complexes of interest are rather large, and thus, DFT calculations are relatively expensive. Consequently, we applied hybrid methods to obtain geometric information and reaction energies. As a test to consider the effectiveness of the hybrid methods, the geometry of Zn(DIEN-(pyr)$_2$)$^{2+}$ was optimized using both the hybrid ONIOM method and a full B3LYP/6-311G(d,p) calculation. Geometry optimization by

both methods results in very similar structures (see Supporting Information). A quantitative comparison of the geometrical parameters leads us to expect that our hybrid calculations obtain bond lengths and angles to within about 2.5 pm (or 1%) and 8.5° (or 8%), in fact not much worse than the error bars on the crystal structure itself.[65]

Although no independent experimental data are available for comparison, we can compare the hybrid and purely QM reaction energies. The B3LYP/6-311G(d,p) reaction energy for the addition of CH_3CN to the $Zn(DIEN\text{-}(pyr)_2)^{2+}$ complex is found to be −48.4 kJ/mol, and that found using the hybrid method is −75.2 kJ/mol. Clearly, the agreement between the reaction energies from the fully QM treatment and ONIOM is not nearly as good as the agreement observed for the geometric parameters. A reaction energy closer to the fully QM value is obtained (−36.4 kJ/mol) if single point energy calculations using DFT are performed on the geometry optimized structures obtained from the ONIOM calculations. In these single point energy calculations, the ONIOM-derived geometries, which are presumed to be accurate, are used to calculate the energies of both the reactant and product complexes using a full QM treatment.

The failure of the ONIOM method to even qualitatively reproduce the full DFT energy difference when identical geometries were considered is troubling. Because the nitrogens in the DFT portion of the ONIOM calculation are treated as NH_3 groups, the detail of the N−Zn interactions may not be adequately represented. This result further leads us to conclude that our partitioning scheme leaves certain complex electronic effects out of our inner layer that are not accurately calculated with the low level theory. Further work will be needed to determine the necessary model chemistry for obtaining results other than geometric parameters with sufficient accuracy.

We proceeded to evaluate geometric parameters using the ONIOM calculations, expecting relatively accurate determinations of the structure of the complex. Calculated reaction energies using ONIOM and single-point energy DFT calculations, on the other hand, have much larger expected error. The magnitudes of the calculated reaction free energies do, however, compare favorably with the experimentally determined reaction free energies for many of the metal complexes.

To help interpret our experimental results, geometry optimizations and energy calculations were carried out for both reactants (i.e., $M(DIEN\text{-}(pyr)_2)^{2+}$ and CH_3CN) and products (i.e., $[M(DIEN\text{-}(pyr)_2)(CH_3CN)]^{2+}$). The crystal structure of $Zn(DIEN\text{-}(pyr)_2)$, which has been determined previously,[65] was used as the starting (i.e., preoptimized) structure for the geometry optimizations of each five-coordinate metal complex. An octahedral structure (O_h) was used as the starting structure in the geometry optimizations of the six-coordinate complexes. In all cases, the highest multiplicity was used to describe the metal's spin state. Full structural information is available in the Supporting Information, including bond lengths and bond angles. Figure 2 shows typical structures for the five- and six-coordinate complexes that are obtained from the calculations.

Table 2. Calculated and Experimental Thermodynamic Parameters for the Reaction of $M(DIEN\text{-}(pyr)_2)^{2+}$ with Acetonitrile

	ΔG_{calcd} (kJ/mol)		
metal center	ONIOM[a]	ONIOM/DFT[b]	ΔG_{expt} (kJ/mol)[c]
Mn	−100.6	−67.9	−64.8 ± 1.4
Fe	−87.3	−63.2	−61.3 ± 1.9
Co	−97.0	−61.2	−56.6 ± 1.9
Ni	−84.9	−53.7	−66.2 ± 1.6
Cu	−75.1	−41.2	−53.6 ± 0.7
Zn	−75.2	−36.4	−52.6 ± 1.8

[a] ΔG calculated using ONIOM alone. [b] ΔG from single point energy calculations using full DFT on the reactant and product optimized structures, which were obtained from ONIOM geometry optimizations. [c] The experimental ΔG values are determined from the experimentally measured equilibrium constants and by assuming a reaction temperature of 300 K, which was the temperature of the vacuum system.

Upon geometry optimization, the five-coordinate complexes adopt geometries that are closer to D_{3h} symmetry (trigonal bipyramidal) than C_{4v} symmetry (square pyramidal). The values of the N1−M−N5 and N3−M−N5 angles are useful for evaluating the tendency of the complexes to favor one of the two geometries. Values close to 120° for both angles are indicative of D_{3h} symmetry, while angles close to 90° and 180° for the N1−M−N5 and N3−M−N5 angles, respectively, are indicative of C_{4v} symmetry. The optimized six-coordinate complexes all adopt an octahedral geometry that is distorted to differing degrees depending on the metal.

The reaction free energies at 300 K in Table 2, obtained from the ONIOM calculations alone, do not compare favorably with the experimental values for reasons suggested above. In fact, the general trend in free energies that we observe is only partially reproduced. Calculations predict that the Ni(II) complex should have a higher reaction free energy than the Mn(II), Fe(II), and Co(II) complexes, while our experimental data show it has the lowest free energy in the series. Aside from the obvious approximations made in any molecular modeling, several sources of error may be acknowledged. First, the π−d interactions mentioned previously are misrepresented; however, this should produce systematic errors across the series of metals and would not be expected to destroy trends. Second, there are as many as eight isomers of each reactant and product complex, related through inversion of the three secondary amines in the $DIEN\text{-}(pyr)_2$ ligand. For example, two isomers of $Ni(DIEN\text{-}(pyr)_2)^{2+}$ are shown in Figure 4. These isomers most clearly differ by the three coplanar groups in the trigonal bipyramidal structure, which are circled in Figure 4. These two isomers differ in energy by 16 kJ/mol. The number of calculations needed to statistically average reaction energies over all isomers for each of the metal complexes is beyond the scope of this work.

A third source of discrepancy could actually be kinetic in origin. Although we believe the reactions reach an equilibrium among all accessible states, at 300 K there may be kinetically inaccessible states that remain unobserved. Perhaps the low experimental free energy for the reaction

(65) Sosa-Torres, M. E.; Ugalde-Saldivar, V. M. *Acta Crystallogr.* **1993**, *C49*, 796−799.

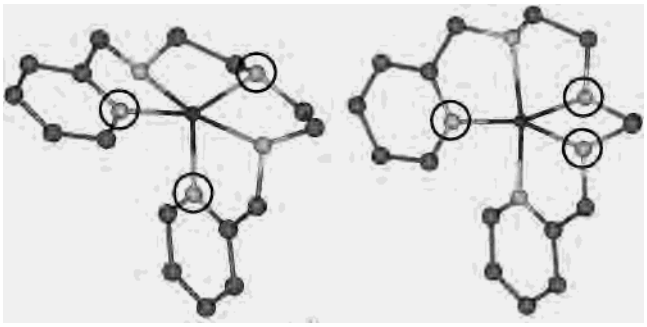

Figure 4. Two isomers of Ni(DIEN-$(pyr)_2)^{2+}$ calculated using the ONIOM method. The circles indicate the atoms that are coplanar in each trigonal bipyramidal structure.

involving Co(DIEN-$(pyr)_2)^{2+}$ could be due to a high barrier, which prevents the lowest energy product from forming. In future work, we will evaluate transition state structures and energies; however, for these simple ligand addition reactions we do not expect large reaction barriers or changes in the spin state of the complexes. In fact, when comparing the measured reaction rate constants with the calculated collision rate constants using the average dipole orientation model,[66] we find that between ~3% (for Zn complexes) and ~15% (for Ni complexes) of the collisions with CH_3CN result in stable product formation. For ions at room temperature, these relatively high reaction efficiencies suggest that the reaction barriers are not very large.

Another factor that could affect the kinetics of these reactions is a radiative contribution to product stabilization. In eq 3, we assume that helium is the sole contributor to product ion stabilization. In actuality, radiative stabilization can also occur, and its propensity might affect reaction kinetics in unexpected ways. We do not, however, expect radiative contributions to play an important role in product ion stabilization because of the relatively high pressure of helium in our experiments. Nonetheless, we have begun to investigate this possibility, and early results suggest that the rate of collisional stabilization exceeds the rate of radiative stabilization by over 2 orders of magnitude, which confirms our expectation.

To summarize the theoretical investigations, we find that the ONIOM embedding approach provides insight into the probable structures of these complexes. Specifically, the five-coordinate complexes are closer to trigonal bipyramidal than to square pyramidal. The predicted reaction free energies are of similar magnitude to those obtained experimentally at 300 K, but quantitative predictions of trends in reactivity are not possible. Fortunately, the geometric information provided can be used in evaluating molecular orbital stabilization energies, which do provide an explanation of our experimental results (vide infra).

AOM Calculations. Given the numerous possible permutations with the ONIOM calculations, stabilization energies from the angular overlap model (AOM) were used as a way to understand the experimental trends. The AOM was developed to describe transition metal−ligand interactions,[67−69] and it can be used to obtain the energy separation of the d-orbitals for any symmetrical complex structure. Using the AOM, molecular orbital stabilization energies (MOSEs) are obtained for the five- and six-coordinate complexes of each metal, and then, the change in MOSE (ΔMOSE), as a function of d^n, is compared with the experimentally determined ΔG values. In determining the MOSE values, the σ-orbital overlap integrals (e_σ) were assumed to be the same for each metal. This assumption should be fairly valid given the identical ligands in each complex and given that systematic differences in e_σ between metals should cancel when reactant MOSE values are subtracted from the product MOSE values. In addition, for the stabilization energy calculations the quartic term of the interaction energy was ignored, and only the quadratic term was considered.

MOSE values calculated by considering both σ and π contributions from the ligands and considering square pyramidal, trigonal bipyramidal, and octahedral geometries are shown in the Supporting Information. The functional groups bound to each of the metals are usually considered strong σ donors, but the pyridine and imidazole rings of DIEN-$(pyr)_2$ and DIEN-$(imi)_2$ can be weak π-donors or π-acceptors and reports have shown that CH_3CN can act as π-donor.[70,71] For the square pyramidal and trigonal bipyramidal complexes, metals with between 5 and 8 d-electrons (i.e., Mn(II) through Ni(II)) can form either high- or low-spin complexes. Literature reports show, however, that five-coordinate complexes containing these metals tend to form only high-spin systems when complexed to ligands having N-containing functional groups. Usually, complexes with weakly electronegative π-donors (e.g., P-containing functional groups) are required to obtain low-spin complexes.[72,73] Nonetheless, both high-spin and low-spin possibilities have been considered for Mn(II), Fe(II), Co(II), and Ni(II), but the MOSE values for only the high-spin cases are listed in the Supporting Information. For the octahedral complexes, Mn(II), Fe(II), and Co(II) can adopt either high-spin or low-spin configurations, and while both possibilities have been considered only the high-spin cases for these metals are listed.

After considering the numerous possibilities of spin states, coordination geometries, and ligand donor contributions, the experimental trend can be now understood. A plot of ΔMOSE values as a function of metal is shown in Figure 5. For clarity, not all the possibilities are included, but rather only those combinations that best explain the experimental trend are plotted. Figure 5 compares the experimental ΔG values (◆ in Figure 5) with the ΔMOSE values for (1) σ

(66) Su, T.; Chesnavich, W. J. *J. Chem. Phys*. **1982**, *76*, 5183−5185.
(67) Jorgensen, C. K.; Pappalardo, R.; Schmidtke, H. H. *J. Chem. Phys*. **1963**, 39, 1422.
(68) Schaffer, C. E.; Jorgensen, C. K. *Mol. Phys*. **1965**, *9*, 401.
(69) Schaffer, C. E. *Pure Appl. Chem*. **1970**, *24*, 361.
(70) Storhoff, B. N.; Lewis, H. C. *Coord. Chem. Rev*. **1977**, *23*, 1−29.
(71) Howell, J. A. S.; Saillard, J.-Y.; Le Beuze, A.; Jaouen, G. *J. Chem. Soc., Dalton Trans*. **1982**, 2533−2537.
(72) Sacconi, L.; Speroni, G. P.; Morassi, R. *Inorg. Chem*. **1968**, *7*, 1521−1525.
(73) Morassi, R.; Bertini, I.; Sacconi L. *Coord. Chem. Rev*. **1972**, *8*, 351−367.

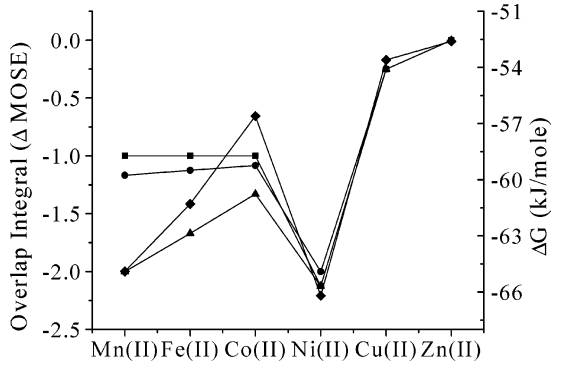

Figure 5. Plots of experimental ΔG values and the overlap integrals from molecular orbital stabilization energy (MOSE) calculations as a function of metal. Experimental ΔG values are represented by the symbol ◆, and the scale for these experimental values is shown on the right-hand side of the plot. ΔMOSE values considering only σ contributions from the ligands are represented by the symbol ■, ΔMOSE values considering both σ and π-donor contributions from the ligands are represented by the symbol ●, and ΔMOSE values considering σ contributions from DIEN-$(pyr)_2$ and a π-donor contribution from CH_3CN are represented by the symbol ▲. The scale for the ΔMOSE values is shown on the left-hand side of the plot.

only contributions from the ligands (■ in Figure 5), (2) σ contributions from DIEN-$(pyr)_2$ and a π-donor contribution from CH_3CN (▲ in Figure 5), and (3) σ and π-donor contributions from all the ligands (● in Figure 5). Because the π-orbital overlap integral (e_π) values are usually much smaller than the e_σ values (i.e., π-bonding is much weaker than σ-bonding), a correction factor is needed to allow a direct calculation of the ΔMOSE values. An arbitrary correction value of 1/12 (e_π/e_σ) was found to qualitatively reproduce the experimental data. For each plot of the ΔMOSE values in Figure 5, a conversion from a high-spin trigonal bipyramidal (D_{3h}) complex to a high-spin octahedral (O_h) complex is shown. None of the other geometric or spin state combinations comes as close to explaining the experimental data. Of course, the five-coordinate complexes of the different metals do not necessarily all have to have the same coordination geometry, but the MOSE values come closest to explaining the experimental data if all the reactant complexes have D_{3h} symmetry.

Close inspection of the data in Figure 5 provides some interesting insight into the reactivity of the complexes. A comparison of the calculated trend using only σ-bonding contributions with the trend calculated using σ- and π-bonding (Figure 5, ■ vs ▲) shows that the octahedral complexes of Mn(II), Fe(II), and Co(II) are stabilized to differing degrees by the π-donor ability of CH_3CN. In fact, the π-donor ability of CH_3CN seems to be responsible for the relatively high reactivity of the Mn(II) complex. If one considers the d-orbital configuration for Mn(II), Fe(II), and Co(II) in the octahedral complexes, the physical reason for this stabilization becomes clear. When placed into an octahedral environmental, the 5 d-orbitals of the metals split into two groups (t_{2g} and e_g orbitals). The t_{2g} orbitals consist of the d_{xy}, d_{xz}, and d_{yz} orbitals, and the e_g orbitals consist of the d_{z^2} and $d_{x^2-y^2}$ orbitals. The t_{2g} orbitals have the appropriate symmetry to allow overlap with the π-orbitals of CH_3CN, and in the case of high-spin complexes of Mn(II), Fe(II), and Co(II) the t_{2g} orbitals are only partially filled. This partially filled character means that these metals can be stabilized by π-bonding whereas the completely filled t_{2g} orbitals of Ni(II), Cu(II), and Zn(II) do not allow stabilization upon π-bonding. Because Mn(II) has only 3 electrons in the t_{2g} orbitals, it can be stabilized the most by π-bonding. This stabilization explains why the Mn(II) complexes are more reactive than the Fe(II) or Co(II) complexes.

One way to test this conclusion experimentally would be to react the complexes in this study with a reagent gas that has no π-donating ability. If π-bonding is important, then the reactivity trend should change when a reagent like NH_3 is used. Unfortunately, NH_3 does not form an adduct with any of the complexes in this study at the typical gas pressures used. This is likely because the enthalpy of this reaction is too low to overcome the unfavorable reaction entropy at room temperature. In fact, to date we have not found a reagent gas devoid of π-bonding ability that simply forms an adduct with M(DIEN-$(pyr)_2)^{2+}$ or M(DIEN-$(imi)_2)^{2+}$ complexes. Reactions of NH_3 with another complex in which the pyridine or imidazole functional groups are replaced by tetrahydrofuran (THF) moieties (i.e., M(DIEN-$(THF)_2)^{2+}$) have been somewhat telling. In this situation, the reaction free energy of the Mn(II) complex of DIEN-$(THF)_2$ is much reduced relative to Ni(II) and becomes similar to the Co(II) complex. Future work will seek to further experimentally confirm the importance of π-donating ability.

Conclusions

Metal complexes containing a first-row divalent transition metal and a pentadentate ligand have been reacted in the gas phase with acetonitrile (CH_3CN). The kinetics and energetics of reagent addition clearly show that these reactions are sensitive to the electronic structure of the complex. The trend in reactivity for the metals with a given ligand is Ni(II) > Mn(II) > Fe(II) > Co(II) > Cu(II) ≈ Zn(II). Both theoretical calculations and the AOM have been employed to understand the reactivity trend. Hybrid calculations using the ONIOM method, in which the metal center and the atoms bound to it are treated at a DFT level and the remainder of the ligand is treated by molecular mechanics, are able to roughly reproduce the experimental trends. Complete quantitative or qualitative agreement between the ONIOM calculations and the experimental data, however, was not possible. This lack of agreement is likely due to the failure to calculate all the potential isomers for both the reactant and product ions. Further optimization of the ONIOM method and consideration of all relevant isomers should lead to better agreement between the calculated and measured values.

The AOM provides a better fit to the experimental data when both σ- and π-bonding are considered. Specifically, only when the π-donor capability of CH_3CN is taken into account can the enhanced reactivity of the Mn(II) complexes be explained and complete qualitative agreement with the experimental data be achieved. Interestingly, both the

ONIOM calculations and the AOM indicate that the five-coordinate complexes react from trigonal bipyramidal or slightly distorted trigonal bipyramidal structures with high-spin-state configurations. These results suggest that ion−molecule reactions may have some potential for gathering insight into the gas-phase coordination geometry of metal complexes. Such information could be used to compare solution-phase or solid-state structures with gas-phase structures, and these comparisons might be telling about the effects of solvent or crystal-packing forces. Finally, the gas phase provides a unique environment in which coordinatively unsaturated and short-lived (e.g., intermediate) complexes can be studied. The potential ability to gather coordination structure information about such complexes could provide some interesting insight into chemical transformations involving divalent metal complexes.

Acknowledgment. M.Y.C. would like to thank the Schering-Plough Research Institute for a summer research fellowship. The authors would also like to thank Thom Vreven and Mike Frisch, both of Gaussian, Inc., for various helpful discussions regarding the ONIOM methodology.

Supporting Information Available: Tables listing bond lengths and bond angles from the ONIOM calculations. Tables with the molecular orbital stabilization energy calculations. This material is available free of charge via the Internet at http://pubs.acs.org.

IC0354668